Filler and Percolation Behavior of Ionic Aggregates in Styrene–Sodium Methacrylate Ionomers†

Joon-Seop Kim, Rebecca J. Jackman,‡ and Adi Eisenberg*

Department of Chemistry, McGill University, 801 Sherbrooke Street West, Montreal, Quebec, Canada H3A 2K6

Received December 3, 1993; Revised Manuscript Received February 21, 1994®

ABSTRACT: The dynamic mechanical properties of poly(styrene-*co*-sodium methacrylate) ionomers were reexamined in detail and the data interpreted in terms of filler and percolation concepts using the Eisenberg–Hird–Moore (EHM) multiplet/cluster model of random ionomers. For this study, samples were synthesized over a wider range of ion concentrations as well as more frequent intervals than in the previous studies. Deconvolutions were performed on the loss tangent data. The glassy moduli of the ionomers were found to be independent of the ion content. There were discontinuities in the plots of the slopes of the storage moduli, peak heights, peak positions, and widths at the half-height of the loss tangent peaks as well as of the activation energies for the glass transitions as a function of ion content. These discontinuities suggest that two morphological changes are involved in the present ionomer system. The first, at 4–6 mol % of ions, involves the formation of a dominant or a continuous phase of the ion-rich or cluster regions and is interpreted as being associated with the percolation threshold (see below). The second, at ~12–14 mol % of ions, possibly involves the disappearance of continuity of the unclustered "phase"; between 4 and 12 mol %, two cocontinuous "phases" are probably encountered. Differential scanning calorimetry (DSC) thermograms for the ionomers between 8 and 14 mol % of ions show two glass transition temperatures (T_g). A linear relation is observed between these two T_gs and the positions of the E'' peaks at 0.3 Hz obtained from dynamic mechanical thermal analysis (DMTA) measurements. In terms of filler concepts, the Guth equation is applicable in the range of low volume fractions of clusters (<0.3), but a minor modification extends the applicability to 0.45. Application of the Halpin–Tsai equation for regular systems to the present ionomer at low ion content suggests that the system consists of more or less spherical (at opposed to linear or lamellar) clusters dispersed in the matrix phase as filler particles. The mechanical properties of ionomers were also interpreted in terms of percolation concepts. At the percolation threshold, i.e., at ~5 mol % of ions, the critical exponent and the critical volume fraction of clusters were found to be 1.31 and 0.64, respectively. The value of the critical exponent is in the range of "universal" values for conductivity percolation, but the critical volume fraction is much higher than those for most other systems. This is explained in terms of the difference between the nonuniformity of properties of the clusters of the present system and the uniformity of properties in usual percolating species. Finally, a novel approach is used to estimate the size of a sodium carboxylate ion pair, which is found to be 45×10^{-3} nm^3.

I. Introduction

Over the past two decades, the morphologies and viscoelastic properties of a wide range of random ionomers have been studied.[1-10] It has been suggested that the ion pairs aggregate to form multiplets and that, at least in some systems, the multiplets may be clustered at sufficiently high ion contents. Several models concerning ionomer morphologies have been proposed, including the core–shell model of MacKnight et al.[12] and the hard-sphere liquid-like interference model of Yarusso and Cooper.[13] The most recent was presented by Eisenberg, Hird, and Moore (EHM),[14] which has unified the interpretations of mechanical properties and morphologies of random ionomers. They suggested that the ionic aggregates or multiplets restrit the mobility of the adjacent polymer chains. With increasing ion content, the restricted mobility regions begin to overlap and eventually from fairly large domains (clusters) which exhibit phase-separated behavior and possess their own T_g. As the ion content increases, the addition of ions causes the size of the clustered region to grow until continuity of the clustered phase is established throughout. In this case, the material can be thought to have achieved (or exceeded) percolation. The change in modulus of the ionomer with ion content would be expected to be related to percolation behavior. One can, of course, also regard the clustered regions as a filler. Thus, one should look at the properties of random ionomers in the light of both filler and percolation concepts.

In the field of rubber processing and technology, the effect of fillers on the mechanical properties of polymers has been explored extensively.[15] Addition of fillers to elastomers can increase the strength and hardness or resistance to deformation of the material; usually, the size and shape of the particles and the degree of dispersion are important factors. One of the most common composites is rubber containing a filler (e.g., carbon black) in quantities up to 20–30% by volume. Two properties of the filler, i.e., the specific surface and the structure, have been accepted as the two most important elements in the quality of a rubber. For instance, the tensile strength of rubber is very strongly affected by differences in surface area or particle size; stiffness and hardness are more dependent on the structure than on the particle size. One of the changes which occurs when a finely divided solid is dispersed in a rubber is stiffening. Guth[16] found that up to a volume fraction of ~0.3 of the filler, the Einstein equation for the viscosity of a suspension can be applied after some modification to take into account higher volume fraction terms. For the equation (given in section E of the Discussion) to be applicable, the fillers should be completely dispersed in the matrix, and the shape of the fillers should be nearly spherical.

* To whom all correspondence should be addressed.
† Based on Chapter 7 of the Ph.D. Thesis of Joon-Seop Kim, McGill University, 1994.
‡ Present address: Chemistry Department, Harvard University, 12 Oxford St., Cambridge, MA 02138.
® Abstract published in *Advance ACS Abstracts*, April 1, 1994.

0024-9297/94/2227-2789$04.50/0

For two-phase systems, e.g., polyblends and block copolymers, attempts were made by Takayanagi[17] and Kaelble,[18] among others, to find the relation between the morphology and the concentration of the two components. They proposed simple models involving connections in series or in parallel of the two components. These models give the highest upper bound and lowest lower bound to the modulus. The equations, which show the relation between the modulus of the composite and those of each component, will be given and discussed in the Discussion. However, these models are too simple to apply to the actual morphology of many real systems. Kerner[19] developed a model in which one of the two components can be thought of as spheres dispersed in a matrix of the other component; phase inversion is also possible. Later, Halpin and Tsai[20] developed equations which cover the whole range of moduli from the lower bound (series connection model) to the higher bound (parallel connection model); these will also be discussed. A useful review of these models is given by Nielsen.[21] With these equations, one can calculate the moduli for different systems which have different morphologies. Therefore, application of these equations to the present ionomers may given some insight into the morphological change of the ionomer as a function of the volume fraction of clusters.

The term percolation for the statistical-geometry model was introduced in 1957 by Hammersley.[22] According to his view, the sites (or bonds) of a lattice can be randomly occupied with a probability p. Percolation concepts deal mainly with the value of the percolation threshold, p_c, at which infinite connectivity of occupied sites (or bonds) first occurs, and the probability of finding such a connectivity as a function of p. In 1973, Kirkpatrick[23] pictured the occupied bonds as conductors and found that just above p_c the conductivity increases according to a power law $(p - p_c)^t$, where t is positive and depends only on the spatial dimension of the lattice. Over the next few years, other physical properties were investigated; it was shown that similar power laws with their own critical exponents existed for particular cases. For instance, the critical exponent is ~0.40 for site percolation,[24-26] ~0.32 for magnetic induction,[24,25] 1.3–2.0 for conductivity,[24-30] ~2.6 for dielectric properties,[30] ~3.8 for the Young's modulus in a sintered silver powder beam system,[31] and ~1.8 for the tensile modulus in blend systems.[32] The percolation concept has been applied to interpret the change in mechanical properties in the transition region as a function of morphology in blends of nylon with rubber by Margolina and Wu[33] and as a function of temperature by Margolina.[34] They showed that the percolation concepts could be applied successfully to analyze the data and explain the transitions. A brief survey of the other studies relating percolation to elastic moduli will be given in the Discussion. In the field of ionomers, no study has been published of mechanical properties interpreted in terms of percolation concepts, and only very few papers exist which apply percolation concepts to conductivity of ionomers and ionomer blends.[28,35-37] Very recent studies have been performed on conductivity in the poly(methyl methacrylate-*co*-cesium methacrylate) [P(MMA-*co*-MACs)] system by Gronowski et al.[36] and some polystyrene-based ionomers by Jiang et al.[37] They found that, in the water-swollen state, the ionomers exhibit a sharp transition from an insulator to a conductor with increasing ion content. Site percolation concepts were applied to those systems to understand the relationship between the structures of those ionomers and the amount of water.

Since the EHM model[14] described the cluster as a high-modulus inclusion, at least at low ion contents, we propose to analyze viscoelastic data in the light of percolation and filler concepts. It should be stressed, however, that the present system, according to the EHM model, does not represent the ionomers as consisting of relatively monodisperse particles embedded randomly in a polymer matrix. Rather, we are dealing with overlapping multiplets which form irregularly shaped clusters (filler or percolating species) which grow in both size and number and simultaneously increase the modulus as their volume fraction increases. The percolation threshold would be expected to be reached when the cluster phase becomes continuous.

Several previous studies on the poly(styrene-*co*-sodium methacrylate) [P(S-*co*-MANa)] ionomers have been carried out, but none of them covered a wide enough range of compositions with small enough intervals to allow the type of analysis proposed here.[38,40] In the earliest study, involving torsion pendulum and stress relaxation techniques, Eisenberg and Navratil[38,39] found that at low ion concentration (up to 6 mol % of ions) time–temperature superposition was obeyed and the WLF equation[41] was applicable. Above 6 mol % of ions, time–temperature superposition was no longer applicable. For the low ion content materials, the matrix T_gs were found to increase approximately linearly with concentration of ions up to 6 mol %. Above that ion content, the matrix T_gs of the material increased faster. The increase in ion content was paralleled by a broadening of the distribution of relaxation times. In all samples of high molecular weight and an ion concentration above 1%, two inflection points were visible on the stress relaxation master curve as well as two peaks in the loss tangent plots. The upper inflection point increased with increasing ion content. It was suggested that below ~6 mol % of ions, the ions existed in the form of simple multiplets, while above that concentration more extensive ion clustering was encountered. Much more recently, Hird and Eisenberg[40] suggested that the relative heights and areas of the loss tangent peaks were associated with glass transitions of the matrix and cluster phases of the P(S-*co*-MANa) system. It was also suggested that the cluster phase becomes dominant and may coalesce into a continuous network at ~6 mol % of ions. In addition, the high activation energies for the high-temperature transitions support the suggestion that the high-temperature loss tangent peak is a true glass transition. Again, however, not enough ion concentrations were investigated to interpret the mechanical properties in terms of filler or percolation concepts.

To apply these concepts to the random ionomer system in the solid state, one needs sets of mechanical property data over a broad concentration range acquired over small intervals of ion concentration. Therefore, it was decided to prepare samples of P(S-*co*-MANa) over a wider ion concentration range and at more frequent intervals than was done before. The conversions were in the range of 3–5% to keep compositional heterogeneity below 0.2. Compositional heterogeneity is defined as [(composition of the first polymer chain) − (composition of the last polymer chain at certain conversion)]/(average composition of the polymer chains). In the present study, the mechanical property measurements were performed by using a dynamic mechanical thermal analyzer (DMTA). Thus, it became possible to determine a wide range of parameters in more detail than in previous examinations; these parameters include (1) the glassy moduli (E'_g), (2) the "ionic" moduli (E'_{ionic}), (3) the rubbery moduli ($E'_{rubbery}$), (4) the slopes of the storage modulus curves as a function of temperature in the region of the matrix glass transition (m_1), the slopes of the "ionic plateaus" (m_{ionic}), the slopes of the storage modulus curves for the cluster glass transition (m_2), and those of the rubbery "plateaus" ($m_{rubbery}$), (5) the activation energies for the matrix glass

transition, for the cluster glass transition, and for ion hopping, and (6) the tan δ peak positions, areas under the peak, widths at the half-height of the peak maxima, and heights of peaks measured at 1 Hz. Furthermore, recently, as a part of an investigation of the molecular weight effect on dynamic mechanical properties, it was found that ionomers of high molecular weight must be investigated to get precise cluster peak information.[42] Therefore, high molecular weight ionomers, i.e., $M_n = \sim 500\,000$, were used in the present work. In addition, small-angle X-ray (SAXS) data, acquired in connection with another project,[37] were utilized for a recalculation of the sizes of multiplets. Finally, a reexamination of the materials by differential scanning calorimetry (DSC) was undertaken.

II. Experimental Section

The synthesis of the P(S-*co*-MANa) ionomers, the sample preparation conditions, and the method of characterization have been described elsewhere.[38,40,42] For convenience, only a brief summary of the procedure is given in section 1 of the supplementary material. The specific reaction conditions along with molecular weights and polydispersity indices of some of the ionomers are given in section 2 of the supplementary material. The sample notation used for the ionomers is P(S-x-MANa), where x is the mole percent of the sodium methacrylate.

Dynamic mechanical property measurements were performed using a Polymer Laboratories DMTA. For each sample, the storage moduli (E'), loss moduli (E''), and loss tangents (tan δ) were obtained in the dual cantilever bending mode as a function of temperature (80–350 °C) at a heating rate of 0.5 °C/min. The experiments were performed at five frequencies ranging from 0.3 to 30 Hz under a dry nitrogen atmosphere. Because of the low precision of the bending mode for storage modulus values $<10^5$ Pa, further DMTA experiments in the shear mode with a sandwich geometry were performed on three low ion content samples to obtain accurate data for the low-modulus region at high temperatures. The experimental conditions were the same as those for the dual cantilever bending mode experiments.

For each sample, mechanical property measurements were carried out at five frequencies; detailed data analysis was, however, only performed on a 1-Hz data. Deconvolutions were performed on loss tangent (tan δ) data using the PeakFit (Jandel Scientific) program. The best fits were achieved assuming an exponential background and fitting the matrix and cluster peaks, generally, with exponentially modified Gaussian peaks. In extreme cases, i.e., very low and very high ion contents, it was necessary to fit the peaks with a Gaussian or sometimes two Gaussian curves. The deconvolutions were carried out over a temperature range from 100 to ~30 °C above the minimum on the high-temperature side of the cluster peak. Recently, it was found that the results obtained using the WLF relation as a background were also reasonable.[42] Therefore, the WLF relation was used as a background to fit the loss tangent data of some of the samples. The results of the deconvolutions are listed in Table B in section 3 of the supplementary material, along with the results obtained by use of the exponential background. It was found that there were only minor differences between these two sets of results. Therefore, the results obtained with the exponential background were used to treat all data (all the equations are given in section 3 of the supplementary material). Table C in section 3 of the supplementary material contains the parameters obtained from these equations. Each parameter was plotted as a function of ion content and fitted with zero-, first-, or second-order polynomials; the equations for these curves are also given in Table C. With the exception of the peak positions, there is no fundamental scientific significance of these parameters. However, the equations are useful, because one can calculate the loss tangent vs temperature curves in the range of ~2–11 mol % for the P(S-*co*-MANa) ionomers without performing any experiments. Figure A in section 3 of the supplementary material shows the best and worst fits calculated using the given equations.

For the thermal analysis studies, a Perkin-Elmer DSC-7 was utilized. The experimental conditions are also given in section 1 of the supplementary material.

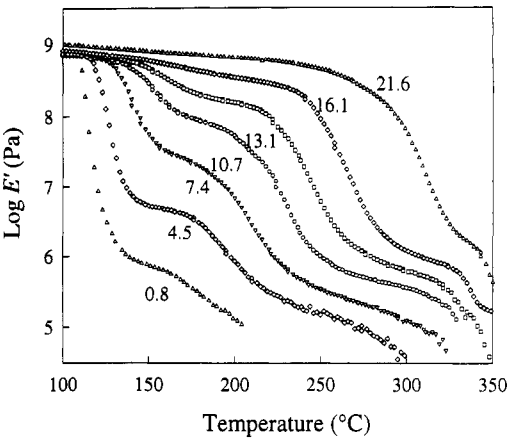

Figure 1. Representative storage modulus (E') plots as a function of temperature for the P(S-*co*-MANa) system with ion contents marked near each plot. All data obtained at 1 Hz.

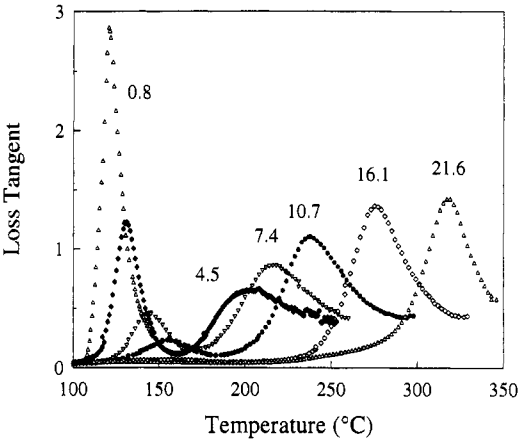

Figure 2. Representative loss tangent (tan δ) plots as a function of temperature with ion contents marked near each curve. All data obtained at 1 Hz.

III. Results

A. Principal Features and Definitions. A series of representative storage modulus (E') and loss tangent (tan δ) curves as a function of temperature, recorded at 1 Hz for a range of P(S-*co*-MANa) copolymer samples, is shown in Figures 1 and 2, respectively. Since for some samples DMTA measurements were carried out in two different modes, i.e., bending and shear, it is important to confirm that results obtained from these two modes yield complementary information. Figure B in section 4 of the supplementary material shows the combined curves of the storage tensile modulus (E') and three times the storage shear modulus (G') as well as the loss tangents (tan δ) for the P(S-2.2-MANa) sample. The results are in excellent agreement.

Figure 3a shows a plot of the storage modulus as a function of temperature for the P(S-6.6-MANa) sample. One can define five domains on this plot; the curve shows clearly two transition regions in which the storage modulus is changing rapidly with temperature, as well as three regions which show a much more gentle decrease in slope, resembling behavior in the region of a plateau. The value of the modulus at the first plateau is described as the glassy modulus (E'_g). In this study, the glassy modulus is defined in two ways: first, as the value of the storage modulus at 100 °C and second, as the value of the modulus at a temperature 40 °C below the first glass transition temperature (as estimated for the tan δ peak position). The first transition region, the slope of which is called m_1, corresponds to the glass transition of the matrix. The intemediate region in which the modulus changes slightly with temperature can be characterized by two parameters,

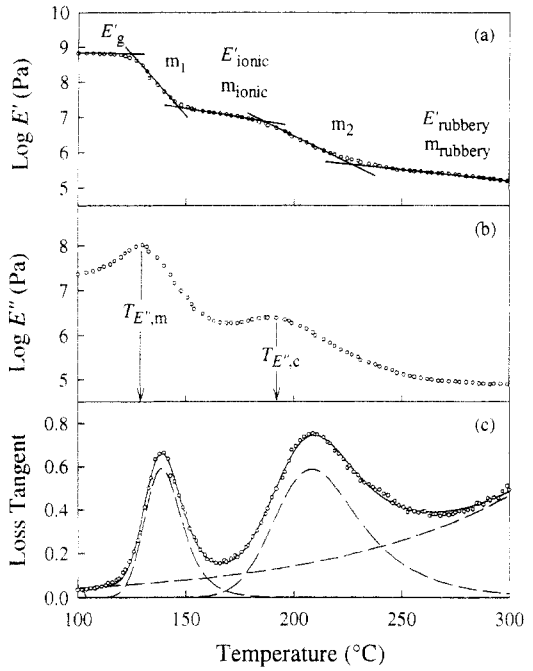

Figure 3. Plots of (a) storage modulus, E', (b) loss modulus, E'', and (c) loss tangent (tan δ) peak for the P(S-6.6-MANa) ionomer as a function of temperature, measured at 1 Hz. The meanings of the various parameters extracted from the data are indicated graphically.

E'_{ionic}, the value of E' at the point of minimum slope, and the slope of the plot at that point, m_{ionic}. This region reflects ionic cross-linking, as discussed extensively before.[40,43] This is followed by a more rapid decrease in the slope, which is labeled m_2, and is associated with the glass transition of the clustered regions. The last region is characterized by a rather gentle decrease in slope. This region is denoted as the rubbery modulus ($E'_{rubbery}$) and the corresponding slope, $m_{rubbery}$. This region is associated with the same phenomena which give rise to a rubbery modulus in nonionic polymers.

A plot of the loss modulus curve for P(S-6.6-MANa) as a function of temperature is shown in Figure 3b. Evident in this plot are two peaks associated with the low- and high-temperature glass transitions, which are due to the matrix and the cluster regions, respectively. The temperatures at the maxima of these peaks are defined $T_{E'',m}$ and $T_{E'',c}$ respectively. For these peaks, apparent activation energies can also be calculated from an Arrhenius plot of log(frequency) vs inverse temperature. Only the $T_{E''}$ values are used in the subsequent analysis.

The loss tangent curve as a function of temperature for the same sample is shown in Figure 3c. It is the matrix glass transition which gives rise to the first peak and the glass transition of the cluster region that is associated with the second peak. The best fit curve for each of the samples was obtained with an exponential background and exponentially modified Gaussians for the peaks. From the deconvolutions, the values for a number of parameters could be obtained. The peak positions, $T_{g,m}$ and $T_{g,c}$, are the temperatures at the maxima of the low- and high-temperature transition peaks, respectively. The values A_m and A_c are the areas under the matrix and cluster peaks, and $\sum A$ is the sum of the areas. The full width at the half-height of the peak is also of interest and is designated as ΔT_m and ΔT_c for the two peaks. Apparent activation energies for each transition, i.e., E_a(matrix) and E_a(cluster), were also calculated from the slopes of the Arrhenius plot of log(frequency) vs inverse temperature for the tan δ peaks, as was also done for the E'' peaks (see above).

B. Detailed Analysis of E' Curves. The glassy modulus (E'_g) is tabulated as a function of ion content in Table D in section 5 of the supplementary material. It is clear from an examination of the data that log E' is essentially constant at 8.90 ± 0.05 (as measured at T = 100 °C) or 8.88 ± 0.06 (as measured at T_g - 40 °C, where T_g is taken as the peak temperature in the tan δ plot at 1 Hz). Thus, within experimental error, the variation of ion content in the range studied here does not affect the glassy modulus.

The slope in the first transition region, m_1, vs ion content is plotted on a semilogarithmic scale in Figure C in the supplementary material. Log m_1 decreases from ~0.7 to ~2.7 as the ion content increases (from 0.0 to 21.6 mol %). There also appears to be a discontinuity in the plot at ~5 mol % of ions.

In the plot of the ionic inflection point (E'_{ionic}) as a function of the ion content (Figure D in the supplementary material), one observes, as would be anticipated, that the value of log E'_{ionic} increases from ~5.9 to ~8.8 with increasing ion content (from 2.2 to 21.6 mol %). At low ion contents, the relation appears linear; however, beginning at ~8 mol %, the points fall below the extrapolated line. At the highest ion contents, the value of the "ionic modulus" approaches the value of the glassy modulus. The segments of the modulus curves which exhibit an ionic plateau are not horizontal but show a slight downward slope. It is of interest to see the variation of the slope with ion content. The values of m_{ionic} are also plotted as a function of ion content in Figure D. While the slope is small, it is clearly increasing with increasing ion content up to a maximum at ~8 mol % and then decreases as the ion content increases further. Also, it should be mentioned that the temperature range over which this ionic "plateau" extends increases with increasing ion content.

In the second transition region, the slope, m_2, again increases from ~0.015 to ~0.060 with increasing ion content (from 0.8 to 21.6 mol %), as can be seen in Figure C in the supplementary material; at the higher ion contents (>12 mol %), a slight curvature is observed.

The rubbery modulus ($E'_{rubbery}$) as a function of ion content is plotted in Figure E in the supplementary material; it is observed that log $E'_{rubbery}$ initially increases linearly with ion content from a value of ~5.1 at 2.2 mol %, exhibits some degree of curvature at higher ion contents, and reaches a value of ~6.0 at 21.6 mol %. Examination of the slope at the rubbery inflection point ($m_{rubbery}$) as a function of ion content (Figure E) shows that up to ~16 mol % it is almost constant at ~0.0075, but then a definite upward trend is seen.

The activation energies for ion hopping can be calculated from the modulus data near the ionic plateau (from the frequency dependence of the intersection of linear segments of the log E' plot), as was suggested by Hird and Eisenberg.[43] Figure F(b) in the supplementary material shows that the activation energies increase from ~220 (for 2.2 mol %) to ~400 kJ/mol (for 10.0 mol %) with increasing ion content. Figure F(b) also shows two more sets of activation energies obtained from the loss tangent (tan δ) maxima and loss modulus (E'') maxima for the high-temperature transition; these will be discussed below. The activation energies for ion hopping can be calculated by this method only up to ~10 mol %, because above that the ion content, irregular features in the log E' vs temperature plot make it very difficult to determine the activation energies. Figure F(b) in the supplementary material shows that identical E_a values are obtained by the three methods up to 10 mol %.

C. Detailed Analysis of E'' Curves. Figure 4 shows the positions of peak maxima from plots of the loss modulus

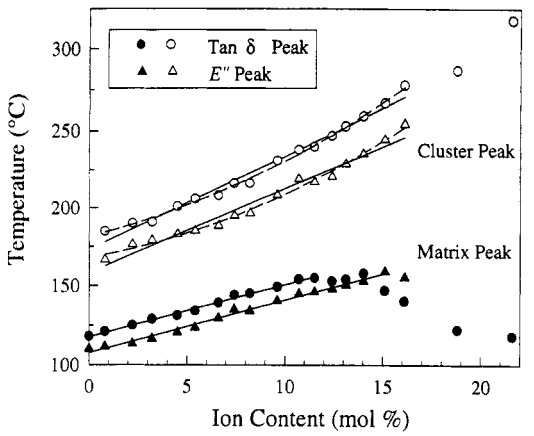

Figure 4. Glass transition temperatures of matrix and cluster regions as a function of ion content, measured at 1 Hz. First- and second-order polynomial fits are also shown.

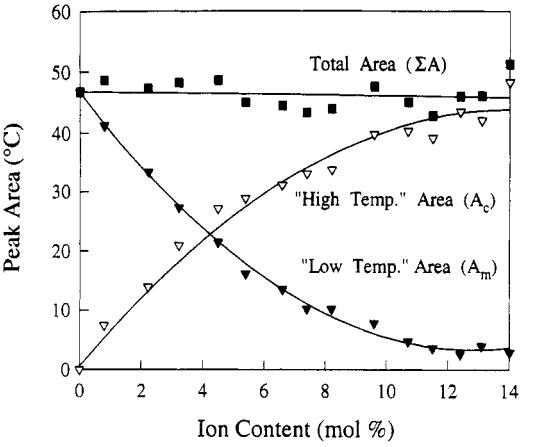

Figure 5. Areas under loss tangent peaks and the sum of the areas as a function of ion content measured at 1 Hz.

against temperature as a function of the ion content. A typical log E'' vs temperature curve was already shown in Figure 3b. The peak temperatures associated with the glass transitions of matrix regions increase, but only up to ~15 mol %; beyond that point, a progressive decrease is observed. In the linear region, data can be fitted with a first-order polynomial. The equation for the matrix peak positions is

$$T_{E'',m} = 108 + 3.3c \quad (r^2 = 0.995)$$

where c is the mole percent of ions and r^2 is the linear least-squares correlation coefficient. The peak positions associated with the cluster regions increase with ion content over the whole range. Data up to 16 mol % were, again, fitted with a first-order polynomial (solid line). Because a slight curvature was seen on the plot, an attempt to fit the data with a second-order polynomial was also made. The equations for the cluster peak positions are

$$T_{E'',c} = 158 + 5.5c \quad (r^2 = 0.985) \text{ (first-order fit)}$$

and

$$T_{E'',c} = 168 + 2.2c + 0.19c^2 \quad (r^2 = 0.996)$$

(second-order fit)

As can be seen in Figure 4, the second-order polynomial (dashed line) gives a marginally better fit. The activation energies from the peak maxima are plotted in Figure F in the supplementary material, which also shows the activation energies obtained from the tan δ peak maxima. Figure F shows that the activation energies for the glass transition of the clusters obtained from E'' plots increase from ~250 (for 2.2 mol %) to ~300 kJ/mol (for 9.6 mol %) with increasing ion content, as did those obtained from the intersections of linear segments in E' plots, and that the values are in very good agreement. For the glass transition of the matrix, it is found that the activation energies increase more gently from ~650 (for ~4 mol %) to ~720 kJ/mol (for ~10 mol %), but then they decrease to ~400 kJ/mol (for ~18 mol %). However, it should be mentioned that at low temperatures, the log E'' curves for the low ion content samples show some irregularities, as do the high ion content samples at high temperatures. These irregularities consist of peak splitting, which makes the calculation of activation energies very risky. Therefore, the activation energies were not calculated for the matrix transition at low ion contents or for the cluster transition at high ion contents.

D. Detailed Analysis of tan δ Peaks. Figure 4 also shows the peak temperatures obtained from the tan δ plots. As for the results from E'' plots, the peak positions associated with glass transition temperatures of the matrix phase increase linearly with ion content; again the data were fitted with a first-order polynomial. The plot of the position of the matrix peak as a function of ion content is also linear up to ~12 mol % of ions; for that region, the equation for the straight line is

$$T_{g,m} = 118 + 3.3c \quad (r^2 = 0.997)$$

Beyond 14 mol %, the glass transition temperature of the matrix peak begins to decrease in parallel with the results from E'' data. At this point, it should be mentioned that in the previous study by Navratil and Eisenberg[38] a discontinuity was observed at ~6 mol % in the plot of $T_{g,m}$ vs ion content; however, in the present study, this behavior is not seen. For the cluster peak positions, the data up to 16 mol % were again fitted with both the first-order (solid line) and the second-order polynomials (dashed line). The equations are

$$T_{g,c} = 173 + 6.1c \quad (r^2 = 0.992) \text{ (first-order fit)}$$

and

$$T_{g,c} = 181 + 3.3c + 0.16c^2 \quad (r^2 = 0.998)$$

(second-order fit)

The second-order polynomial, again, gives a marginally better fit. If one compares the first-order fits for both temperatures, one finds that the rate of increase of the glass transition temperature for the cluster transition is almost twice as high as that for the matrix transition.

The average of the total area under the peaks for the samples up to 14 mol % was measured to be 47 ± 2 °C. The areas under the matrix (A_m) and cluster peaks (A_c) and the total area (ΣA) are shown in Figure 5. Only results for samples with ion contents up to 14 mol % were plotted, since at higher ion contents the curve fitting for the matrix peak became inaccurate and meaningless. The data for the areas under the matrix and cluster peaks as a function of ion content were fitted with second-order polynomials. For the matrix peak the equation of the best fit curve is

$$A_m = 47 - 6.8c + 0.26c^2 \quad (r^2 = 0.999)$$

and for the cluster peak

$$A_c = 6.2c - 0.22c^2 \quad (r^2 = 0.995)$$

These values are useful to demonstrate the smooth transition from the dominance of the matrix peak to that of the cluster peak, since the peak areas can be regarded as a measure of the volume fraction of the clustered or unclustered material, both being essentially polystyrene.

In Figure G in the supplementary material, the peak width at half-height is plotted as a function of ion content. The width of the peak associated with the clustered material (ΔT_c) becomes narrower (from ~65 to ~30 °C) with increasing ion content. The matrix peak width (ΔT_m), by contrast, increases linearly (from ~15 to ~35 °C) up to ~14 mol % of the methacrylate, at about the same rate as the cluster peak decreases; at 14 mol %, the increase becomes much greater, i.e., to ~60 °C, and at 15 mol %, the width seems to level off at ~70 °C.

In Figure H in the supplementary material, the peak heights are plotted on a semilogarithmic scale as a function of ion content. As would be expected, with increasing ion contents, the matrix peak height becomes smaller (from ~0.5 at 0 mol % to ~−1.5 at 21.6 mol % on a logarithmic scale) as the clustered material begins to dominate; concurrently, the cluster peak increases in height. The logarithm of the cluster peak height increases linearly with ion content up to ~14 mol % (from ~0.5 at 0.8 mol % to ~0.0 at 21.6 mol %), but the change in height is less dramatic than that for the matrix peak. There is, clearly, a smooth transition from a system with a dominant unclustered phase to one with the clustered phase dominating.

The activation energies of the glass transition for the matrix and cluster regions, calculated using Arrhenius plots, are shown in Figure F in the supplementary material. The activation energies for the cluster transition increase with ion content from ~200 (for 2.2 mol %) to ~600 kJ/mol (for 21.6 mol %), but for the matrix transition they increase slowly from ~550 (for 2.2 mol %) to ~650 kJ/mol (up to 10 mol %) and then decrease rapidly to ~300 kJ/mol (for 21.6 mol %) with increasing ion contents.

IV. Discussion

A. The Glassy State. One would expect, intuitively, that the presence of ionic groups should raise the glassy modulus. However, in the present system, it is shown that, within experimental error, the glassy moduli do not change with increasing ion content (Table D in the supplementary material). This suggests that the reduction in the mobility due to the presence of ionic aggregates, which is so important in the glass transition region, does not manifest itself when the temperature is substantially below the glass transition of both the matrix and the cluster regions. The isochronal or constant-frequency storage modulus reflects the chain mobility of the polymer, i.e., the chain dynamics, at a certain temperature. In the glassy state, the dynamics of polymer chain segments are of very short range. The short-range chain dynamics in the matrix phase and in the cluster phase are apparently very similar and are not appreciably affected by the presence of multiplets.

It should be also mentioned that the volume fraction of multiplets, which will be discussed below, is ~6% for the 21.6 mol % ionomer. In this temperature range, if one takes the multiplet as a filler particle, one can apply the Guth equation[16] to calculate the storage modulus of the ionomers in the glassy state. If this equation is applicable to the 21 mol % sample, then E'_g(ionomer)/E'_g(polystyrene) = 1.20; thus, the difference in storage moduli of these two polymers is only 0.080 on a logarithmic scale. This value is small and close to the experimental error. Also, the difference between the E' of the glassy polystyrene and that of the multiplet is not necessarily large, and thus the small volume fraction of multiplets may not affect the glassy modulus by as much as calculated by the Guth equation. An alternate application of the Guth equation will be discussed below in connection with the view of clusters as filler particles at temperatures above the glass transition.

Table 1. Ion Contents at Which Discontinuities or Maxima Are Observed

feature	Figure	discontinuities or maxima at ion content (mol %)
m_1	Figure C	5
E'_{ionic}	Figure D	8
m_{ionic}	Figure D	8
m_2	Figure C	12
$m_{rubbery}$	Figure E	16
E_a for matrix transition	Figure F	~10
$T_{g,m}$ (from tan δ)	Figure 4	14
matrix peak width at half-height	Figure G	14
cluster peak width at half-height	Figure G	4
intersection of A_c and A_m	Figure 5	4
cluster peak height	Figure H	4
matrix peak height	Figure H	14

B. Relation between Morphology and Mechanical Properties. After analyzing the sets of data obtained in this study as a function of ion content, it is found that there are discontinuities or maxima in the plots at certain ion contents, e.g., at ~4–6 mol % and at ~12–14 mol %, which are listed in Table 1. From the presence of these discontinuities or maxima in the plots of the observed data, supported by the EHM model, one may draw some morphological and other conclusions about the P(S-*co*-MANa) ionomers as a function of ion content. These conclusions are summarized below.

As was suggested in the EHM model, at very low ion contents, i.e., below ~4 mol %, as one introduces ionic groups into polystyrene, the ion pairs form multiplets surrounded by polymer with restricted mobility; the relative volume of the regions of restricted mobility grows with increasing ion content. In addition, the matrix phase becomes more heterogeneous. This process can be thought to be similar to the introduction of cross-links or filler particles into the polymer, which effectively increases the modulus of the materials with increasing cross-link density or filler content.[43] This is especially true once clusters begin to form, since one can now view the clusters as filler particles. At ~4–6 mol %, the cluster phase becomes dominant, or even continuous.[40] In the range of 6–12 mol % of ions, it seems reasonable to suggest the existence of two cocontinuous phases, i.e., cluster and matrix. As the ion content increases, the clusters increase in size, and the volume fraction of cluster phase becomes bigger, while that of the matrix phase becomes smaller. At very high ion contents, i.e., above 12 mol %, the cluster phase, which now occupies >90 vol %, has probably become the only continuous phase in the systems, and its homogeneity increases progressively. At that high ion content, the nature of the matrix region also changes from one that essentially resembles normal polystyrene at low ion content to a material which exists on the surfaces of the clusters or in the small regions between clusters. Therefore, it is not surprising that the nature of the matrix phase should be very different from what it is at very low ion contents. Perhaps it might be useful to compare the situation discussed here with what one finds when one compares the amorphous phase in a highly crystalline polyethylene, in which it is located at the surfaces of the lamellae, with that found in molten polyethylene.[44] The nature of two amorphous materials is very different.

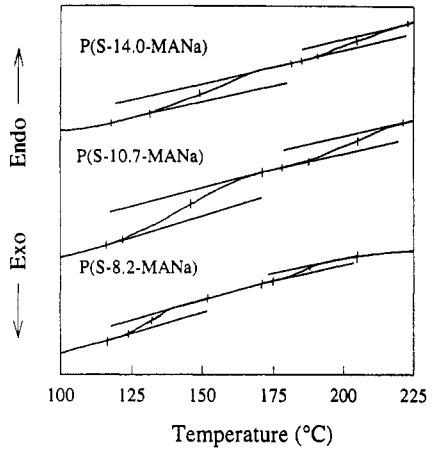

Figure 6. DSC thermograms for the 8.2, 10.7, and 14.0 mol % samples.

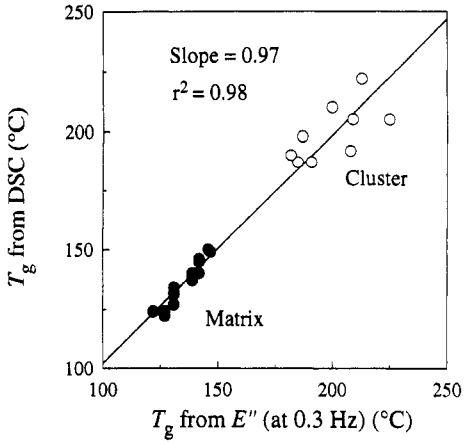

Figure 7. Comparison of the glass transition temperatures obtained from loss modulus (E'') at 0.3 Hz and DSC for matrix and cluster regions.

C. Two Glass Transition Temperatures. In this paper, as in a number of preceding articles, it was suggested that the high-temperature peak represents the glass transition of the cluster phase. This suggestion, however, has not received universal acceptance. This is due, in part, to the fact that the detection of both T_gs by DSC on the same sample is not generally possible, although it has been successful in two cases, i.e., for a sulfonated ethylene–propylene–ethylidenenorbornene (S-EPDM) ionomer studied by Maurer[45] and for a poly(ethylacrylate-*co*-sodium acrylate) ionomer studied by Tong and Bazuin.[46] In the present system, both glass transitions can also be seen by DSC, as shown in Figure 6. The curves show two glass transitions, which are completely reproducible for the second scan, for the samples of ion contents of 8.2 and 14.0 mol %. In addition, the sample which contains 10.7 mol % of ions was scanned four times, with all of the scans giving idential results. However, it should be noted that for samples which were heated to very high temperatures, i.e., 280–300 °C, only one T_g was observed. At this point, we do not have any explanation for this behavior. However, it is not unusual for thermal treatments to change the DSC profiles of polymers.[45] It is noteworthy that for the materials which show two T_gs by DSC, i.e., 8–14 mol %, the volume fractions of the cluster phase are 0.77–0.94, respectively. On the other hand, for the samples of 6 mol % or less, which contain at most 70% of clustered material, the second glass transition is not seen at all in the DSC thermograms. In view of these volume fractions, the values of the heat capacity change (ΔC_p) are puzzling.

From an examination of the series of loss modulus curves (not shown), it is seen that even at very low ion contents, i.e., ~0.8 mol %, a second peak is present which is not observed in the homopolystyrene sample. This is, obviously, due to the glass transition of the cluster regions. It is surprising that it already appears at such a low ion content. This must mean that at 0.8 mol % of ions the material contains coordinated multiplets which form clusters in the sense of the EHM model.

There is a linear relation between the two loss modulus maxima measured by DMTA at 0.3 Hz (ascribed to matrix and cluster T_gs) and the T_gs measured using DSC (Figure 7). The same kind of linearity was also observed in other ionomer systems, i.e., poly(styrene-*co*-sodium acrylate) [P(S-*co*-AANa)], poly(styrene-*co*-cesium acrylate) [P(S-*co*-AACs)], and poly(vinylcyclohexane-*co*-sodium acrylate) [P(VCH-*co*-AANa)].[47] However, it should be mentioned that in those systems, only one DSC glass transition curve was observed for all samples, which represented the glass transition of the dominant phase only, i.e., either the matrix or the cluster phase. In the present system, in the range of 8–14 mol % of ions, both T_gs are seen by both techniques.

At this point, it is useful to review some of the other observations which show that the two transitions in the ionomer systems are both glass transitions. First of all, as was mentioned above, the dynamic mechanical property measurements show that the second loss tangent peak is a glass transition peak. This has been suggested before by Hird and Eisenberg,[40] among others. In addition, in the study by Kim et al.[47] the comparison of the storage modulus curve as a function of temperature for polystyrene with that of the P(S-29.6-AACs) ionomer showed that the shapes of curves are very similar to each other and that the loss tangent peaks exhibit similar activation energies. It should be stressed that polystyrene is a one-phase material containing only the unclustered phase, while the P(S-29.6-AACs) ionomer is also essentially a one-phase material containing the clustered phase. Therefore, the decrease in the storage modulus in the range of the glass transition in polystyrene is due to only the matrix phase, and in the P(S-29.6-AACs) it is due to only the cluster phase. At intermediate ion contents both T_gs are seen, which are found to vary with temperature in a systematic way (see Figure 4). This continuity of behavior for both transitions suggests that the cluster transition is a real glass transition, just as real as it is in unclustered polystyrene.

The preferential plasticization of the clustered region of an ionomer also suggests that there are matrix and cluster phases which have their own T_gs. Recently, in the study by Kim et al.,[48] it was shown that when sodium sulfonated polystyrene ionomers were mixed with sodium *p*-dodecylbenzenesulfonate, the surfactant molecules plasticized mainly the clustered regions and thus affected only the upper T_g. This surfactant molecule has a head group identical to the ionic group of the polymer chain. The incorporation of surfactant head groups into the multiplets is responsible for the preferential plasticization of the clustered regions, since the tail groups reside in the regions of restricted mobility surrounding the multiplets. This causes a large decrease in the glass transition temperature of the cluster phase as a function of added surfactant, with only a slight effect on the T_g of the matrix phase.

The addition of nonpolar plasticizer to the ionomers is also relevant. It has been shown that both the matrix phase and the cluster phase are platicized, resulting in an essentially parallel drop in the two T_gs.[49] If the upper tan δ peaks were due, for example, to the spontaneous breakup of multiplets, it is unlikely that the effect of the plasticizers of low polarity on this process would be the same as it is on the low-temperature glass transition.

Two glass transitions as detected by techniques other than dynamic mechanical measurements were also found

in an ionomeric material based on poly(tetrafluoroethylene) (Nafion). For the Nafion system, it was found by Takamatsu and Eisenberg[50] that there are two discontinuities in the volume vs temperature curves. It was suggested that the upper discontinuity correlates with the cluster T_g of the material, while the lower one is found in the vicinity of the mechanical β-dispersion of that polymer, i.e., the matrix T_g.

Activation energies of the two transitions are revealing. In this context, however, it is useful to discuss also the possible mechanism of the upper T_g. It has been suggested that this mechanism involves a superposition of ion hopping or bond interchange and simple chain motion.[43] Hird and Eisenberg found that in the poly(styrene-*co*-sodium styrenesulfonate) [P(S-*co*-SSNa)] ionomer system, ion hopping is, indeed, involved in the glass transition and that the activation energies for the ion-hopping process remain constant with ion content at ~190 kJ/mol.[43] It is known that in the sulfonates the interaction between ion pairs in the multiplet is relatively strong, and thus the ion hopping process does not occur at reasonable frequencies until a high temperature is reached.[43] Kim et al.[48] found that the activation energies for the glass transition of the cluster phase in the sulfonated polystyrene ionomers also remain constant with ion content at ~200 kJ/mol, which is similar to those for the ion hopping. Also, the glass transition temperature of the cluster phase of P(S-*co*-SSNa) occurs at temperatures much higher than the glass transition temperature of the matrix phase. Therefore, the ion hopping process occurs far above the glass transition temperature of the matrix phase. At that high temperature, the chain motion is very rapid and thus does not contribute to the activation energy for the glass transition of the cluster phase. By contrast, in the case of the P(S-*co*-MANa) ionomer, the glass transition temperature of the cluster phase occurs much closer to the matrix T_g than in the P(S-*co*-SSNa) ionomer. This is due to the fact that in the methacrylates the electrostatic interaction between the ion pairs in the multiplet is weaker than that in the sulfonates. Therefore, the activation energy of the glass transition of the cluster phase in the methacrylate system reflects not only ion hopping but also a contribution from the chain motion. The glass transition of the cluster phase in the sulfonates occurs at much higher temperatures than in the methacrylates, yet the activation energies for the glass transition process are lower for the cluster phase of the sulfonates than the methacrylates. Thus, it is seen that the glass transition temperatures are related to the strength of electrostatic attraction between the ion pairs in the multiplets but show no direct relation to the activation energies.

Bond interchange or ion hopping as a glass transition mechanism is well known. It is encountered in materials such as the network glasses, e.g., SiO_2 or P_2O_5. The difference between these materials and the P(S-*co*-MANa) ionomers is that in the latter both mechanisms, i.e., ion hopping and chain dynamics, contribute significantly to the glass transition of the cluster phase.

D. Size of Ion Pairs and Volume Fractions of Multiplets. In the following two sections, the mechanical properties of the P(S-*co*-MANa) ionomers will be discussed in view of filler and percolation concepts. The filler effect or percolation behavior will be discussed as a function of the volume fraction of the cluster phase or that of the multiplets or of the mole percent of ions. The volume fraction of the cluster phase can be obtained from the areas under the loss tangent peaks. To use the volume fraction of multiplets as one of the variables, one needs to evaluate the size of the multiplet; this aspect is discussed below.

To calculate the size of multiplets, it is assumed that the ionic core contains only ionic groups, which are sodium carboxylate pairs in this system. It is not possible to obtain direct information about the size of the multiplets or, for that matter, about the effective sizes of the sodium carboxylate pairs in the ionomer. However, an indirect method of evaluation is available. One starts with an examination of the densities,[51] the formula weights, and the number of atoms in the structure of some common inorganic compounds which resemble multiplets, i.e., sodium carbonate, sodium bicarbonate, sodium formate, sodium hydroxide, sodium acetate, and sodium oxalate. Using this information, one can calculate the average size per atom in these systems. The results are given in Table 2. The average volume per atom is remarkably constant, equal to $(11.3 \pm 0.5) \times 10^{-3}$ nm^3. This constancy is surprising. However, once it is noted, the average value can be utilized to calculate the volume of the sodium carboxylate ion pair in a multiplet. Thus, the volume of one sodium carboxylate ion pair (4 atoms/ionic group), is $\sim 45 \times 10^{-3}$ nm^3. It is worth noting that this information allows one to calculate the density of the multiplets to be ~2.5 g/cm^3.

The treatment outlined above can also be applied to the hydrocarbons, i.e., the styrene units and the methacrylate units without the sodium carboxylates. The average atomic volume can again be calculated from the densities[52] and molecular weights of some common polymers, i.e., polystyrene, polyethylene, polypropylene, etc.; the number of atoms per repeat unit is obviously known. The results are also given in Table 2. The calculation shows three types of average volumes. First, the average atomic volume for the hydrocarbon polymers is $(9.4 \pm 0.5) \times 10^{-3}$ nm^3 (Table 2). The second value is $(10.3 \pm 0.9) \times 10^{-3}$ nm^3 for the polymers containing oxygen and/or nitrogen atoms. The last is the overall average atomic volume and is calculated to be $(9.8 \pm 0.9) \times 10^{-3}$ nm^3. With these numbers, one can calculate volumes and volume fractions of multiplets in ionomers for which densities are unavailable.

For the present system, three different methods were used to calculate the volume of hydrocarbon units without the sodium carboxylate units. The first utilized the densities of the P(S-*co*-MANa) ionomers determined by Arai and Eisenberg,[53] from which volume fractions could be calculated directly. It should be mentioned, however, that the density values are available only up to ~10 mol %. Thus, one needs to extrapolate the data to get densities at high ion contents. The data were fitted with a first-order polynomial, which gave the density as $1.05 + 0.004x$ mol % of ions. For example, for the P(S-20.0-MANa) sample, the extrapolated density of the ionomer is 1.13 g/cm^3. One can now calculate the volume fraction of multiplets. One considers 100 mol of repeat units of the ionomer, which contain 80 mol of polystyrene units and 20 mol of sodium methacrylate units; the weight of this ionomer sample is 10480 g. From the density, the volume of this ionomer can be calculated to be 9274 cm^3, while the total volume of the ion pairs is 542 cm^3 ($=45 \times 10^{-3}$ nm^3 $\times$ 20.0 $\times$ Avogadro's number); thus, the volume fraction of multiplets is 0.058, assuming that all ion pairs are in multiplets. In the second approach one chooses the average atomic volume of polystyrene, i.e. 10.4×10^{-3} nm^3, and that of polypropylene, i.e., 9.2×10^{-3} nm^3, to calculate the volume of the styrene units and that of the methacrylate unit without the carboxylate, respectively. Again, the volume of sodium carboxylate is chosen to be 45×10^{-3} nm^3. In this case, the volume fraction of multiplets for the 20 mol % sample is also 0.058. The last attempt involves a calculation based on the overall average atomic

Table 2. Volume per Atom of Various Salts and Polymers

salt	form wt	density (g/cm³)	no. of atoms per equiv	vol per atom (×10⁻³ nm³)
sodium hydroxide	40.0	2.13	3	10.4
sodium formate	68.0	1.92	5	11.8
sodium bicarbonate	84.0	2.16	6	10.8
sodium carbonate	106.0	2.53	6	11.6
sodium acetate	82.0	1.53	8	11.1
sodium oxalate	134.0	2.34	8	11.9
			av	11.3 ± 0.5

polymer	mol wt of repeat unit	density of polymer (g/cm³)	no. of atoms per repeat unit	vol per atom (×10⁻³ nm³)
polyethylene	28.1	0.86	6	9.10
polypropylene	42.1	0.85	9	9.15
polystyrene	104.2	1.04	16	10.4
polyisoprene	68.1	0.91	13	9.53
1,4-*trans*-polybutadiene	54.1	0.97	10	9.26
1,4-*cis*-polybutadiene	54.1	1.01	10	8.90
1,2-polybutadiene	54.1	0.96	10	9.36
	hydrocarbon polymers av			9.4 ± 0.5
poly(ethylene terephthalate)	192.2	1.34	22	10.9
poly(methyl methacrylate)	100.1	1.19	13	10.7
poly(vinyl acetate)	84.1	1.19	12	10.0
poly(acrylonitrile)	53.1	1.18	7	10.7
poly(butylene terephthalate)	216.2	1.30	24	11.5
polyamide 6 (amorphous)	113.2	1.09	19	9.08
polyamide 66 (amorphous)	226.3	1.09	38	9.08
	O- and/or N-containing polymers av			10.3 ± 0.9
	overall av			9.8 ± 0.9

volume of polymers, i.e., 9.8×10^{-3} nm³. Using this number, one can calculate the volume of the hydrocarbon units without multiplets. Since the volume of multiplets is known from above, one obtains 0.060 as the volume fraction of multiplets. There are only marginal differences between these three volume fractions, even at such a high ion content. Therefore, for this study, only the first method using extrapolated densities is used to calculate the volume fraction of multiplets.

E. Clusters as Filler. It is possible to interpret the mechanical properties of ionomers by considering either multiplets or clusters as filler particles. It should be noted, however, that for the ionomer which contains 15 mol % of ions, the volume fraction of the cluster phase is ~0.95, while the volume fraction of the multiplets is only ~0.05. Above an ion content of ~15 %, the mechanical properties of ionomers do not change much with increasing ion content, because ionomers already are composed mainly of a clustered material. However, the volume fraction of multiplets increases linearly with increasing ion content in that range and beyond. Thus, the mechanical properties of ionomers are more closely related to the volume fraction of clusters than to that of multiplets. Therefore, in the first part of the present section, only the cluster phase will be considered as filler. Subsequently, for the sake of completeness, calculations will also be performed for multiplets as filler.

One of the early relations between the Young's modulus and the concentration of filler is given by the Guth equation,[16]

$$E^* = E(1 + 2.5V_f + 14.1V_f^2)$$

where E^* is the Young's modulus of the filled system, E is that of the unfilled system, and V_f is the volume fraction of filler. For spherical particles, this equation is applicable up to ~30 vol % of filler. In the case of ionomers, one can take the ionic modulus, E'_{ionic}, as E^*; the rubbery modulus of polystyrene is then taken as the Young's modulus of the unfilled polymer, and the volume fraction of clusters as the volume fraction of filler. If this is done, it is found that in the range of low volume fraction of clusters, i.e., up to ~0.3, the data are in good agreement with the Guth equation. This is shown in Figure 8. The dotted line represents a modified equation which will be discussed below. Above 30 vol % of clustered material, the ionic clustered modulus increases dramatically and shows deviations between experimental data and calculated values.

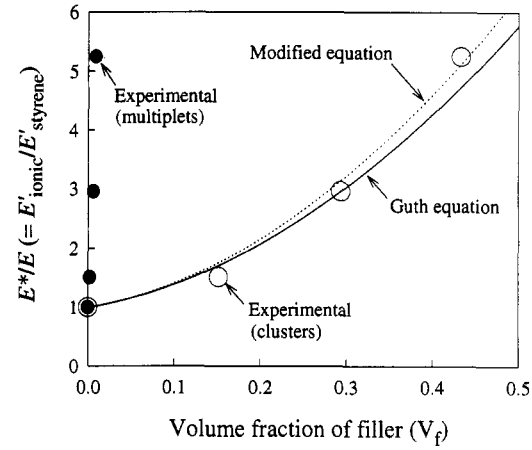

Figure 8. Ratio of the moduli vs volume fraction of filler. The solid line represents the Guth equation, and the dotted line shows the modification of the Guth equation. The unfilled and filled circles represent the data for the volume fraction of clusters and of multiplets, respectively.

An attempt was made to fit data points beyond 30% with a modified Guth equation. To do so, only the second term was allowed to vary, keeping the first term, 2.5, constant. This procedure allowed the extension of the fit to ~45 vol % of clustered material. This modified equation is

$$E^* = E(1 + 2.5V_f + 16.2V_f^2) \quad (r^2 = 0.990)$$

and is also shown in Figure 8 as the dotted line. Naturally, further modification could be attempted but would necessitate the introduction of additional terms which would probably be meaningless.

In block copolymers or polyblend systems, the relationship between the elastic moduli, the composition of the

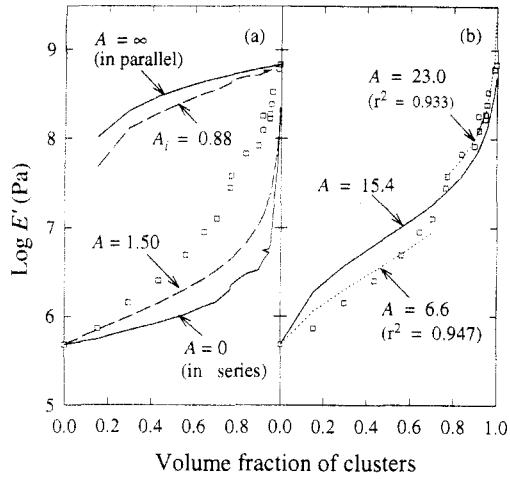

Figure 9. Ionic moduli vs volume fraction of clusters. (a) Solid lines represent the model involving connections in series or in parallel of two components by Takayanagi, and dashed lines for the calculated values for the regular and inverted systems by Halpin and Tsai. (b) Solid line represents the calculated moduli using the regular system, and the two dotted lines indicate the calculated values for two separate regions, i.e., below and above the volume fraction of 0.7. The squares represent the observed experimental data.

two components, and the morphologies has been studied extensively. One of the simplest models involves connections in series or in parallel of the components, and gives the highest upper bound or the lowest lower bound for the modulus.[17,18] The highest upper bound of the modulus is given by

$$M = M_1\varphi_1 + M_2\varphi_2$$

where M is the modulus of the material, M_1 and M_2 are the moduli of components 1 and 2, and φ_1 and φ_2 are the volume fractions of components 1 and 2, respectively. This equation is applicable to the sample in which two components are connected in parallel to the direction of the applied force. The lowest lower bound of the modulus is obtained from the model in which two components are connected in series, perpendicular to the applied force; the equation is given by

$$1/M = \varphi_1/M_1 + \varphi_2/M_2$$

In the present system, the moduli for the upper and the lower bounds were calculated. For the calculation, polystyrene was considered as component 1 and P(S-21.1-MANa) ionomer was taken as component 2. Because the 21 mol % ionomer is composed almost exclusively of clustered material with the volume of the matrix phase <1%, it is reasonable to consider this ionomer as only clustered material, i.e., as component 2. Therefore, it was reasonable to suggest that in pure polystyrene there was no clustered material and thus that φ_1 was 1 and φ_2 was 0. In the 21 mol % ionomer, again, because there is only a trace of the unclustered material as determined by the area under the tan δ peaks, the volume fraction of the clustered material, φ_2, was assumed to be 1, which gave φ_1 = 0. The storage moduli were taken from the rubbery modulus of polystyrene and the "ionic modulus", E'_{ionic}, of the ionomer. The calculated moduli are shown in Figure 9a, which also shows moduli calculated using other equations. The calculated moduli from the parallel and the series (perpendicular) models do not fit the experimental moduli of the real systems, which implies that these models are too simple for the present case. However, it is useful to show these two extreme cases in Figure 9a for the purpose of comparison with other cases which will be discussed below. It should be noted that the calculated lines are not smooth, because the experimental areas under the peaks were taken as a volume fraction of clusters, and the moduli were calculated for those values.

At this point, it is useful to discuss other models which are closer to real systems. For the model in which rigid spheres are dispersed in the elastomeric phase, the so-called regular system, the modulus of the material can be calculated using the Halpin–Tsai equation.[20,21,54]

$$\frac{M}{M_1} = \frac{1 + AB\varphi_2}{1 - B\varphi_2}$$

and

$$B = \frac{M_2/M_1 - 1}{M_2/M_1 + A}$$

In this equation, which is a simplification of Kerner's equation,[19] M is the modulus of the material and the subscripts 1 and 2 refer to the continuous phase and the dispersed phase, respectively. M_1 was taken from the rubbery modulus of polystyrene at 155 °C, i.e., $E' = 10^{5.68}$ Pa. M_2 was taken to be the ionic modulus of the 21 mol % ionomer at 195 °C, i.e., $E' = 10^{8.83}$ Pa. The constant A is strongly dependent on the morphology of the material and can be described by

$$A = k - 1$$

where k is the Einstein constant. The value of the constant A is generally given by

$$A = \frac{7 - 5\nu_1}{8 - 10\nu_1}$$

where ν_1 is Poisson's ratio for the matrix. To calculate the modulus for the regular system, the matrix was considered to be polystyrene in the rubbery state at ~160 °C. Poisson's ratio of polystyrene in the rubbery state was taken to be the same as that of natural rubber at room temperature, 0.50,[52] yielding A = 1.50. The result for the calculation is shown in figure 9a, along with that for the inverted system. The fit is unsatisfactory.

For the system in which the rigid phase is continuous with soft elastomeric spheres dispersed in the rigid phase, i.e., the so-called inverted system, the above equation can be changed to that below[20,21,54]

$$\frac{M_1}{M} = \frac{1 + A_iB_i\varphi_2}{1 - B_i\varphi_2}$$

and

$$B = \frac{M_1/M_2 - 1}{M_1/M_2 + A_i}$$

where $A_i = 1/A$ and the subscript 2 refers to the dispersed phase, i.e., the low-modulus phase. However, one cannot get direct information about Poisson's ratio of the cluster phase. For the inverted system, the continuous phase, i.e., the cluster phase, is more rigid than the elastomeric filler (i.e., the polystyrene phase) and the viscoelastic property of the cluster phase in the temperature range between the T_gs is similar to that of polystyrene in the glassy state. Thus, Poisson's ratio was assumed to be 0.325 (giving A_i = 0.88). The calculated moduli for the inverted systems are also shown in Figure 9a. The fit is still unsatisfactory.

From Figure 9a, it is clearly seen that below 80 vol % of the clustered material, the experimental data are closer to the calculated values for the regular system than to those for the inverted system. It should be mentioned that above the phase inversion, specifically for the range 0.6 < volume fraction of clusters < 0.8, the ionic moduli of ionomers are still far below the calculated moduli of the inverted system. This means that, in that range, the present ionomer system can be still considered as a regular system. However, the ionic moduli increase rapidly as the volume fraction of clusters increases, and above a volume fraction of clusters of 0.8, the experimental modulus values are closer to the calculated moduli for the inverted system. However, at no point does the system become inverted. This means that even at a high volume fraction of clusters, the matrix phase cannot be considered as consisting of spherical particles of the matrix material dispersed in the continuous cluster phase. By contrast, at low volume fractions of clusters, the clustered material does seem to be dispersed as more or less spherical particles (i.e., irregular isolated clusters) in the matrix phase.

The constant A is dependent on the dimensions and geometries of the filler particles. Usually, fillers can be divided into three classes. The first class is one-dimensional, e.g., fibers, whiskers, etc. The second is two-dimensional, e.g., ribbon, flakes, platelets, etc. The last is three-dimensional, e.g., beads, spheres, etc. Again, the A value is related to the Einstein coefficient, k. It is known that the Einstein coefficient changes with the morphology of the material.[54] For instance, for spheres which form aggregates, the Einstein coefficient increases with increasing number of spheres per aggregate. Also, if the filler is in the shape of a rod, the Einstein coefficient increases with increasing length to axis ratio. In the case of uniaxial fibers or ribbon-like fillers, the Einstein coefficient, in general, varies from 1 to infinity, depending on the ratio of the length to the diameter for the fiber or of the width to thickness ratio for the ribbon.

Since the constant A can vary between zero (series model) and infinity (parallel model) as the morphology of the material changes, it is of interest to inquire how the present ionomers fit into the above scheme. Considering the system as a regular system, one may wish to fit all the data with a single value of A; the best result is shown in Figure 9b, with $A = 15.4$. This is not a good fit for any particular region. It is much more reasonable to fit the data with more than one equation. It can be seen that below ~70 vol % of clusters, the moduli calculated from $A = 15.4$ are higher than the experimental moduli, while above ~70 vol % the experimental moduli are higher than the calculated moduli. Thus, based on this curve, one can divide the data points into two regions, i.e., low volume fraction (<0.70) and high volume fraction (>0.70) of clusters, and one can try to fit the data with two separate curves for these two separate regions. After fitting the data, two values for the constant A are obtained as 6.6 ($r^2 = 0.947$) and 23.0 ($r^2 = 0.933$) for the region of the low and high volume fraction of clusters, respectively. It should be mentioned that for reasonable fitting through the data in the region of high volume fraction, the two data points of highest volume fraction (>0.975) were omitted. If the reinforcing species were to consist of unassociated spheres (e.g., isolated multiplets with their surrounding restricted mobility regions), the constant A should be in the range 1–1.5 (for the regular system $A \sim 1.5$). However, the A values which were obtained here are much higher than that. This means that in this ionomer system, the filler is, most likely, in the form of highly irregular aggregates, as the clusters were postulated to be.[14] Furthermore, the change in the constant A from ~7 to ~23 suggests that the number of aggregates per cluster increases with increasing volume percent of clusters; naturally, geometrical and dimensional changes are also involved.

Lewis and Nielsen[55] showed that for large aggregates the maximum packing fraction can vary from 0.64 for random close packing to 0.52 for simple cubic packing. The corresponding maximum values of the Einstein coefficient, k, would be 3.9 (giving $A = 2.9$) and 4.8 (giving $A = 3.8$), respectively. In the present system, however, even the constant A for the low volume fraction region, i.e., 6.6, is higher than those of Lewis and Nielsen. Again, this is not surprising, because for the present system the size of filler particles (clusters) is not uniform and the shapes of the filler particles are not spherical.

An attempt was also made to see whether it is reasonable to regard multiplets as filler in the region between the two glass transition temperatures. The volume fractions of multiplets were calculated using the information given in section D of the discussion. The results are also shown in Figure 8 as filled circles. The concept is obviously not valid, since the points are very far from the line of the Guth equation. Thus, multiplets cannot be regarded as a filler above the matrix glass transition, but clusters do exhibit very reasonable filler behavior. It is particularly noteworthy that the volume fraction of clusters was taken directly from the area under the loss tangent peak. The behavior observed here reinforces the view of clusters as described in the EHM model.

F. Ionomer Morphology in the Light of Percolation Concepts. In typical percolation plots, the logarithm of the modulus, or any other relevant property, is a linear function of the logarithm of the volume fraction of the percolating species, f, minus the critical volume fraction, f_c. Therefore, if percolation is operative in the present system, a plot of $\log E'$ vs $\log(f - f_c)$ should give a straight line with a slope n. The slope represents the critical exponent for an equation in the form of a power law.

Before the relevant values for this plot can be calculated, one needs the volume fractions of the percolating moieties. However, in the present ionomer system, one cannot define *a priori* what should be regarded as the percolating species, since either clusters or multiplets (with some amplification factor to compensate for the impossibility of contacts between them) could be the percolating moieties involved. Thus, one needs to know the volume fraction of both multiplets and clusters. On the basis of the information about the size of an ion pair (i.e., 45×10^{-3} nm^3/ion pair) which was mentioned before, one can calculate the volume of multiplets in the ionomer. Again, it is assumed that all the ion pairs form multiplets. The volume fraction of clusters is obtained from the area under the loss tangent peaks. With these two volume fractions, i.e., those of multiplets and clusters, and the mole fraction of ions, one can plot $\log E'_{\text{ionic}}$ vs $\log(f - f_c)$, where f can be either the volume fraction of multiplets, the volume fraction of clusters, or, for the sake of completeness, the mole fraction of ions. From the latter, one obtains the value of the ion concentration at the percolation threshold.

The critical concentrations (i.e., volume fraction or mole fraction) and slopes are obtained by preparing a series of plots of $\log E'_{\text{ionic}}$ vs $\log(f - f_c)$, in which the critical concentration, f_c, is changed systematically. For each of these plots, one calculates the slope and the linear least-squares correlation coefficient. The slope and the critical concentration are chosen for the plot for which the linear least-squares correlation coefficient shows the best value. It should be mentioned that, because the percolation concepts are applicable above but not too far from the percolation threshold, one needs to choose the range of the volume fraction data so as to avoid regions of very

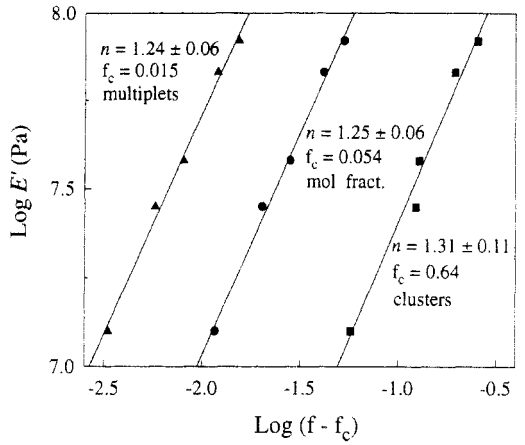

Figure 10. log E'_{ionic} vs log(volume fraction of multiplets, mole fraction of ions, or volume fraction of clusters minus critical concentration at the percolation threshold). n represents the slope of the line, i.e., the critical exponent, and f_c is the critical concentration.

high volume fraction of percolating species. The linear regression function also serves as a criterion for the selection of the upper limit. This is done by a systematic elimination of the highest modulus values until the point is reached where no significant changes in the slope are observed on further elimination of experimental points. This point is reached at ~10 mol % of ions (volume fraction of clusters ~0.90).

Figure 10 shows the best plot of log E' vs log$(f - f_c)$. It is seen that the slope is 1.24 ± 0.06 for f as multiplets, 1.25 ± 0.06 for f as a mole fraction of ions, and 1.31 ± 0.11 for f as clusters. The critical thresholds for those three cases are, respectively, 1.5 vol % of multiplets, 5.4 mol % of ions, and 64 vol % of clusters.

A discussion will now be presented of the critical values, i.e., critical exponent and critical concentration for the system. First, the critical exponent will be considered. The exponent n is considered a universal constant which is applicable to any percolating system and which depends only on the spatial dimensions. Ideally, it does not depend on the morphology, structure, or chemical, mechanical, or statistical properties of the system. For instance, n values for conductivity in a 3-dimensional percolating system were reported to be in the range 1.3–1.7.[24-30,36,37] For example, in recent studies of conductivity in water-equilibrated P(MMA-*co*-MACs) ionomers by Gronowski et al.[36] and several polystyrene-based ionomers performed by Jiang et al.,[37] it was found that with increasing ion content the ionomers exhibit a sharp transition from an insulator to a conductor. Percolation concepts were applicable, and the critical exponents were in the range 1.3–1.7 and critical volume fractions were in the range 0.13–0.16. It should be recalled, however, that, as was mentioned in the Introduction, different critical exponents have been found for different cases, i.e., conductivity, magnetism, or mechanical properties.[24-26] In the following part of the discussion, only the critical exponents obtained from the studies of mechanical properties of materials will be considered, since these are most relevant to the present work.

Many different critical exponents were reported, and those values, in general, belong to three ranges. The first contains the values obtained from the theoretical prediction and from experimental studies of inorganic system; the values are in the range of ~3–4. For example, for the 3-dimensional face-centered cubic lattice, Feng and Sen[56] showed that the exponent should be 4.4 by using the central-force elastic bond percolation model. Kantor and Webman[57] predicted that in the bond-bending model of elasticity of the 3-dimensional lattice-based bond percolation model, the "elasticity" exponent is 3.55. For inorganic systems, Deptuck et al.[31] showed that for sintered, submicron silver powder beams, in the plot of the logarithm of Young's modulus vs log$(f - f_c)$, where f is the occupied volume fraction, the critical exponent is 3.8, while f_c is equal to 0.062. Also Benguigui[58] found 3.5 as the "elasticity" exponent in the 2-dimensional system of metal and voids. In 1986, these critical exponents along with other exponents, which are in the range 3.3–4.0 were tabulated by Sahimi.[59] Later, Forsman et al.[60] also found that in the silica smoke system the critical exponent is 2.9 and f_c ~ 0.017.

The second family contains the values for the polymeric gel systems, with the exponents in the range of ~2–3. For instance, Gauthier-Manuel and Guyon[61] found 1.9–2.2 as exponents in polymerization of a gel of mono- and bisacrylamide. Adam et al.[62] found 3.2 as an exponent for polycondensation and 2.1 for radical copolymerization in the plot of elasticity vs reaction time. Tokita et al.[63] found that the exponent for the dynamic shear modulus of casein gel is 1.9.

The last group contains the values for organic polymeric blend systems for which the exponents are in the range 0.4–1.8. Margolina and Wu[33] found that in the brittle–tough transition in Nylon/rubber blends the exponent is ~0.45 and critical stress volume fraction is ~0.42. Hsu and Wu[32] showed that in the blend system of an amorphous thermoplastic polyester (PETG) and ethylene–propylene–diene rubber (EPDM) the plot of the logarithm of the tensile modulus vs log$(f - f_c)$, where f is the volume fraction of PETG, shows 1.8 as a critical exponent and 0.11 as a critical concentration.

It is interesting to compare the critical exponents for the present system to those in the above three groups. In the present system, all three critical exponents (which fall in the range 1.24–1.31) are in the range of the universal values for the conductivity (1.3–1.7) and are also in the range of the critical exponents for the organic polymeric blend systems. In this respect, the present ionomers resemble the polymer blend percolating system. This is not unreasonable, because in the present system, one deals with the mechanical properties of two materials, i.e., the unclustered and the clustered regions, which are the same in their chemical structure (they are both polystyrene) but different in chain mobility and modulus. This will be discussed in more detail below.

At this point, a discussion of the critical volume fraction is in order. For bond and site percolations on a variety of lattices, the critical concentrations (f_c) are in the range 0.12–0.43 depending on the type of lattice in 3-dimensional space.[24] However, unlike the critical exponents, extrinsic factors such as the interaction between matrix and percolating species, dispersion type, and particle parameters, i.e., size, shape, distribution, and orientation, can affect f_c.[24,29] For example, f_c increases with the surface tension and the adhesive strength of the polymer. Also, f_c depends on the filler structure and morphology; e.g., highly structured and extended fillers offer a larger effective volume and thus lower the threshold.[29] In addition, if the aggregates of filler particles are spread out into a continuously extended network, f_c becomes smaller; on the other hand, if clusters penetrate into several well-isolated regions, f_c becomes larger.[27] Also, for the case in which the sizes of the percolating species are polydisperse, f_c is greater than for the monodisperse case.[33,64] In the present system, the critical volume fraction of clusters is 0.64. This value is much higher than those for the classical percolation systems. The reason for this high value may

be related to the morphology of the present ionomer system, as discussed below.

The bond percolation model deals with connections via bond, while the site percolation model deals with the continuity involving sites, e.g., marbles. The present ionomer system should, therefore, be considered not as a bond percolation model but as a site percolation model. It is useful to recapitulate the principal aspects of the simplest site percolation ideas for convenience. At a very low fraction of filled sites, the sites are filled randomly, but the number of filled sites is not large enough for aggregates to form. It should be stressed that the sizes of the filled sites are all the same. As the fraction of filled sites increases, i.e., as more sites become filled, the filled sites begin to interconnect and to form aggregates. With increasing fraction of filled sites, more filled sites become interconnected to form bigger aggregates. However, it should be stressed that the size of the filled sites still remains constant.

It is very clear that, as applied to the present system, the EHM model is very different conceptually from the classical site percolation model. In the present ionomer system, at very low ion contents, the ion pairs form multiplets which are surrounded by regions of restricted mobility. Also there is some variation in the size of the multiplets, which are randomly dispersed in the matrix phase. It is tempting, at this point, to suggest that the multiplets are the percolating species which occupy the sites. As the ion content increases, new multiplets form at new sites. However, most of these new multiplets form near existing multiplets, yielding coordinated multiplets. The regions of restricted mobility start overlapping and forming clusters. The SAXS profiles for this ionomer system show that the intermultiplet distances are practically independent of the ion content.[37] In general, intermultiplet distances are slightly longer than the loopback distance of the ionomer, which is defined as the preferred intermultiplet spacing which gives rise to the X-ray peak. As the ion content increases, some new clusters form at new sites, but, more importantly, the sizes of the existing clusters increase but with a high degree of irregularity. As the ion content increases still further, the probability of forming new multiplets at new sites becomes very low, but the sizes of the existing clusters increase further. Thus, in the last concentration range, the total number of particles does not increase very much, but their sizes do increase to become the continuous phase. This is the point at which one can expect to reach the percolation threshold, not as the result of an increasing number of particles but as a result of an increase in their sizes at a relatively constant number density. As the ion content increases beyond the percolation threshold, one would expect the number of independent clusters to drop; eventually the whole sample might consist of a relatively small number of clusters with local defects (the unclustered regions). The picture given above is obviously not classical site percolation.

One additional factor needs to be considered. In classical percolation, it is assumed that the properties of the percolating species are uniform throughout. However, even for a single multiplet with a layer of restricted mobility, it has been postulated that the mobility of the chain segment changes as a function of the distance from the ionic aggregate. It is impossible to translate this concept into a modulus picture, because the modulus of a 3-nm particle of variable chain mobility is nebulous. It is only when a sufficient number of multiplets are in close proximity that one can speak of a modulus of the clusters. However, the modulus certainly varies as a function of the distance from the surface of a cluster. Thus, one would expect that the modulus at the surface of a cluster should be appreciably lower than that of regions well inside the cluster and, furthermore, that it should also vary with the size of the multiplet and cluster. Therefore, we are not talking about the percolation of spheres of uniform properties placed on some well-defined lattice but of irregularly shaped particles which grow, and which eventually overlap, but the properties of which change in the process. Therefore, it is not surprising that the critical volume fraction and critical exponent are not exactly those found in other mechanical property studies. The critical volume fraction of 0.64 seems high by comparison to 0.11 (PETG/EPDM system)[32] and 0.41 (Nylon/rubber system)[33] but becomes more acceptable if one considers that the cluster is softer at or near the surface than on the inside but that a modulus measurement averages these differences. The critical exponent of 1.31 seems remarkably close to that for conductivity percolation, perhaps because the "contacting" of clusters is not entirely dissimilar from the onset of conductivity. It is also similar to that for percolation in some blends.[32] Most importantly, the fact that a straight line is obtained on the plot of log E' vs $\log(f - f_c)$ suggests that percolation concepts may be applicable to the present system.

As a part of the present study, critical mole fractions of ions and critical volume fractions of multiplets were also obtained. Clearly, the ion content, multiplet formation, and clustering are three parameters which are related to one another. The critical value of 1.5 vol % of multiplets is not very revealing. Multiplets, which are the ionic aggregates without any polymeric material, are clearly not contacting each other when percolation occurs. It does illustrate, however, the profound effect that a small volume fraction of ionic material exerts on its surroundings. It is clear that if one compares the volume fraction of clusters and that of multiplets at the percolation threshold, one can find that the ratio of the volume of clusters to that of multiplets is ~40 (=64/1.5). In view of this large effect, it is worth inquiring why comparable effects are not seen in normal filler systems. The reason becomes clear when one realizes that common filler particles have dimensions as large as 100 μm,[15] while the size of multiplets is of the order of 1 nm. Thus, the size of filler particles can be orders of magnitude larger than that of multiplets. If one were to prepare filler particles of the order of 1 nm in diameter which are dispersed in the polymer at distances of 2–3 nm and which interact with the polymer chains surrounding them through primary chemical bonds rather than via physical interactions, one would probably see the immobilization effect.

Figure 10 suggests that there is a discontinuity (percolation threshold) at 5.4 mol % of ions. The range of 5–6% coincides with a large number of discontinuities in mechanical properties, i.e., in the slope of the storage modulus curve in the range of the glass transition of matrix phase (m_1), the cluster tan δ peak width and height, and the equality of the areas under the matrix and the cluster tan δ peaks. In addition, in the previous study by Navratil and Eisenberg,[38] stress-relaxation and water uptake data showed a discontinuity in this range. All these phenomena can now be interpreted as occurring at or near the percolation threshold.

V. Summary and Conclusions

In this study the effect of the ion content on the mechanical properties of P(S-*co*-MANa) ionomers was reinvestigated in detail, and some of the results were interpreted in the light of filler and percolation ideas. The range of ion contents was broader and the concentration

intervals between samples were smaller than in the previous investigations. Also, several parameters were investigated which were not looked at in the previous studies. Many of the findings, naturally, agree in general with the previous results, but more details are provided here. In addition, however, a number of new insights have been gained, and these are emphasized below.

The Glassy State. The glassy modulus is independent of the ion content. This phenomenon can be understood if it is recalled that the temperature range in which the glassy modulus was measured is far below the matrix glass transition temperature. Therefore, dynamics of the chains are of very short range and are apparently not affected by the presence of multiplets. It should be recalled that the total volume percent of multiplets is very small (it equals approximately the mole percent of ions divided by 3). In this temperature region, the multiplets themselves can be regarded as a filler in a glassy matrix of polystyrene. Since their volume fraction is low, the effect of the T_g is also low.

Relation between Morphology and Mechanical Properties. In addition to a number of parameters which had been measured before, i.e., moduli, positions and heights of tan δ peak maxima, areas under the peaks, activation energies, etc., several parameters were evaluated for the first time for this system. These include m_1, m_2, $m_{rubbery}$, m_{ionic}, activation energies from E'' maxima and those for ion hopping, positions of E'' maxima, and widths at the half-height of tan δ peaks. The slopes of storage modulus curves associated with matrix and cluster transitions plotted as a function of ion content show discontinuities at ~5 and at ~12 mol %. Also, there are discontinuities in the plots of the slopes related to the ionic and rubbery moduli as a function of ion content at ~8 and ~16 mol %. In addition, the plots of the loss tangent peak widths at the half-height, matrix peak positions, and peak height vs ion content also show discontinuities at around 4 and 14 mol %. These results suggest that phase inversion (continuous network formation) occurs in the range of 4–6 mol % and that the high-temperature phase becomes, for all practical purposes, the only material at ~12–16 mol %. The apparent activation energies for the cluster transition and ion hopping increase linearly with increasing ion content. However, those for the matrix transition increase up to 10 mol % and then decrease rapidly. This is probably due to a change of the nature of the matrix phase. The activation energies obtained by different methods show very good agreement.

Two Glass Transition Temperatures. DSC thermograms of the samples which contain 8–14 mol % of ions show clearly that there are two glass transitions associated with the matrix and cluster phases. Other arguments are presented or reviewed which reinforce the view that both these features and the tan δ peaks are indeed glass transitions. There is a linear relation between temperatures of E'' maxima obtained by DMTA at 0.3 Hz and the T_gs measured by DSC.

Size of Ion Pairs and Volume Fractions of Multiplets. Using physical property data of inorganic compounds which resemble the species in the ionic core, the average size per atom for such systems was calculated to be $(11.3 \pm 0.5) \times 10^{-3}$ nm^3. Thus, the size of one sodium carboxylate ion pair was calculated to be 45×10^{-3} nm^3. Using this volume, the density of multiplets was calculated to be 2.5 g/cm^3. By using a similar procedure, the average size of an atom in the hydrocarbon units of polymers was calculated to be $(9.4 \pm 0.5) \times 10^{-3}$ nm^3 for hydrocrbon polymers and $(10.3 \pm 0.9) \times 10^{-3}$ nm^3 for polymers containing oxygen and/or nitrogen atoms; the overall average atomic size was calculated to be $(9.8 \pm 0.9) \times 10^{-3}$ nm^3. Some of these data, along with densities of the ionomers from the literature, were used to calculate the volume fraction of multiplets.

Clusters as Filler. Application of the filler concepts to this ionomer system showed that the Guth relation is applicable up to 30 vol % of clusters. A modification of the Guth equation was applicable up to 45 vol % of clusters. An attempt to use multiplets only as filler was unsucessful, since the experimental points are very far from the theoretical curve. This shows that in the temperature region between two glass transitions, clusters are the only species which can be regarded as filler particles, not multiplets.

Other filler models were used to explore the relationship between the cluster content and mechanical properties. First of all, simple models involving connections in series or in parallel of the two components were used to fit the data, but the calculated moduli did not fit the experimental values. This implies that these models are too simple. The Halpin–Tsai equation was used to calculate the modulus for regular and inverted systems. The Poisson's ratio of polystyrene was used to calculate the contant A of the equation involved. At low ion contents, the shape of the Halpin–Tsai plot is consistent with a picture of more or less spherical filler particles (clusters) dispersed in the unclustered material. By contrast, at a high volume fraction of clusters, the matrix phase does not seem to consist of spherical particles dispersed in the continuous cluster phase. Because the constant A of the Halpin–Tsai equation can vary between zero and infinity, an attempt to fit the data with one single value for A was tried. This was unsuccessful. However, it was found that one can get good agreement if one fits the data with two separate curves for two separate regions above and below 70 vol % of clusters. The two A values are 6.6 (volume fraction of clusters <0.70) and 23.0 (>0.70). These values are much higher than those of Lewis and Nielsen. This is not surprising, because in the present system, the sizes of filler particles are not the same and the shapes of filler particles are not spherical.

Ionomer Morphology in Light of Percolation Concepts. To apply percolation concepts to these bulk random ionomers, a log–log plot was prepared of the E'_{ionic} against the volume fraction of percolating species minus critical volume fraction. Both multiplets and clusters were taken as the percolating species. The slopes, i.e., critical exponents, and the critical concentrations were obtained as 1.31 ± 0.11 and 0.64 for the volume fraction of clusters, 1.24 ± 0.06 and 0.015 for the volume fraction of multiplets, and 1.25 ± 0.06 and 0.054 for the mole fraction of ions. The critical exponent values are in the range of universal values for conductivity percolation and are also similar to those for moduli of some blends. However, the critical concentration for the clusters is higher than those obtained from elasticity studies of percolating systems.

These results can be rationalized by considering the change in the number of multiplets and in the size of clusters as a function of ion content as well as the difference in mobility or modulus in different regions of the clusters. Therefore one should not expect the critical values at the percolation threshold of this ionomer system to be the same as those for classical site percolation. On balance, it appears that percolation concepts may be applicable to the present system with a critical exponent of 1.31 and critical volume fraction of clusters of 0.64. The percolation threshold is located at a mol percent of ions of 5.4, which coincides with a wide range of discontinuities in mechanical and other physical properties.

Acknowledgment. This work was supported by the Natural Sciences and Engineering Research Council of Canada (NSERC).

Supplementary Material Available: Synthesis and characterization of P(S-*co*-MANa) ionomers and the sample preparation conditions; table of specific reaction conditions, along with molecular weight; peak fitting equations; table of PeakFit results obtained from the exponential function and the WLF equation background; table of parameters and equations obtained from the deconvolution of the tan δ peaks and figure of the best and worst fits; figure of the comparison of shear and bending mode data; table of the glassy modulus; discussion of the relationships between mechanical properties (especially discontinuities) and morphology of ionomers as a function of ion contents; and figures connected to the topic (24 pages). Ordering information is given on any current masthead page.

References and Notes

(1) Holliday, L., Ed. *Ionic Polymers*; Applied Science Publishers: London, 1975.
(2) Eisenberg, A.; King, M. *Ion-Containing Polymers, Physical Properties and Structure*; Academic Press: New York, 1977.
(3) Eisenberg, A., Ed. *Ions in Polymers*; Advances in Chemistry Series 187; American Chemical Society: Washington, DC, 1980.
(4) Wilson, A. D.; Prosser, H. J., Eds. *Developments in Ionic Polymers*; Applied Science Publishers: New York, 1983; Vols. 1, 2.
(5) Eisenberg, A.; Bailey, F. E., Eds. *Coulombic Interactions in Macromolecular Systems*; ACS Symposium Series 302; American Chemical Society: Washington, DC, 1986.
(6) Pineri, M.; Eisenberg, A., Eds. *Structure and Properties of Ionomers*; NATO ASI Series 198; D. Reidel Publishing Co.: Dordrecht, Holland, 1987.
(7) Bazuin, C. G. In *Multiphase Polymers: Blends and Ionomers*; Utracki, L. A., Weiss, R. A., Eds.; ACS Symposium Series 395; American Chemical Society: Washington, DC, 1989; Chapter 21.
(8) Lantman, C. W.; MacKnight, W. J.; Lundberg, R. D. In *Comprehensive Polymer Science*; Allen, G., Bevington, J. C., Eds.; Pergamon Press: Oxford, 1989; Vol. 2, Chapter 25.
(9) MacKnight, W. J.; Earnest, T. R., Jr. *J. Polym. Sci., Macromol. Rev.* **1981**, *16*, 41.
(10) (a) Tant, M. R.; Wilkes, G. L. *J. Macromol. Sci., Rev. Macromol. Chem. Phys.* **1988**, *C28*, 1. (b) Mauritz, K. A. *J. Macromol. Sci., Rev. Macromol. Chem. Phys.* **1988**, *C28*, 65. (c) Fitzgerald, J. J.; Weiss, R. A. *J. Macromol. Sci., Rev. Macromol. Chem. Phys.* **1988**, *C28*, 99.
(11) Eisenberg, A. *Macromolecules* **1970**, *3*, 147.
(12) MacKnight, W. J.; Taggart, W. P.; Stein, R. S. *J. Polym. Sci., Polym. Symp.* **1974**, *45*, 113.
(13) Yarusso, D. J.; Cooper, S. L. *Macromolecules* **1983**, *16*, 1871.
(14) Eisenberg, A.; Hird, B.; Moore, R. B. *Macromolecules* **1990**, *23*, 4098.
(15) Mark, H. F.; Othmer, D. F.; Overberger, C. G.; Seaborg, G. T., Eds. *Encyclopedia of Chemical Technology*; Wiley-Interscience: New York, 1980.
(16) Guth, E. *J. Appl. Phys.* **1945**, *16*, 20.
(17) Takayanagi, M. In *Mem. Fac. Eng. Kyushu Univ.* **1963**, *23*, 41.
(18) Kaelble, D. H. *Trans. Soc. Rheol.* **1971**, *15*, 235.
(19) Kerner, E. H. *Proc. Phys. Soc. London* **1956**, *B69*, 808.
(20) (a) Halpin, J. C. *J. Compos. Mater.* **1969**, *3*, 732. (b) Halpin, J. C.; Kardos, J. L. *Polym. Eng. Sci.* **1976**, *6*, 344.
(21) Nielsen, L. E. *Mechanical Properties of Polymers and Composites*; Marcel Dekker: New York, 1974; Vol. 2.
(22) Hammersley, J. M. *Proc. Cambridge Philos. Soc.* **1957**, *53*, 642.
(23) Kirkpatrick, S. *Rev. Mod. Phys.* **1973**, *45*, 574.
(24) Zallen, R. *The Physics of Amorphous Solids*; John Wiley & Sons: New York, 1983.
(25) Deutscher, G.; Zallen, R.; Asdler, J., Eds. *Percolation Structures and Processes*; Annals of the Israel Physical Society; Israel Physical Society: Jerusalem, Israel, 1983; Vol. 5.
(26) Stauffer, D. *Introduction to Percolation Theory*; Taylor and Francis: London, 1985.
(27) Cohen, M. H.; Jortner, J.; Webman, I. *Phys. Rev. B* **1978**, *17*, 4555.
(28) Hsu, W. Y.; Barkley, J. R.; Meakin, P. *Macromolecules* **1980**, *13*, 198.
(29) Hsu, W. Y.; Holtje, W. G.; Barkley, J. R. *J. Mater. Sci., Lett.* **1988**, *7*, 459.
(30) Benguigui, L.; Yacubowicz, J.; Narkis, M. *J. Polym. Sci., Polym. Phys. Ed.* **1987**, *25*, 127.
(31) Deptuck, D.; Harrison, J. P.; Zawadzki, P. *Phys. Rev. Lett.* **1985**, *54*, 913.
(32) Hsu, W. Y.; Wu, S. *Polym. Eng. Sci.* **1993**, *33*, 293.
(33) Margolina, A.; Wu, S. *Polymer* **1988**, *29*, 2170.
(34) Margolina, A. *Polym. Commun.* **1990**, *31*, 95.
(35) (a) Hsu, W. Y.; Giri, M. R.; Ikeda, R. M. *Macromolecules* **1982**, *15*, 1210. (b) Hsu, W. Y.; Gierke, T. D.; Molnar, C. J. *Macromolecules* **1983**, *16*, 1947. (c) Hsu, W. Y.; Berzins, T. *J. Polym. Sci., Polym. Phys. Ed.* **1985**, *23*, 933.
(36) Gronowski, A. A.; Jiang, M.; Yeager, H. L.; Wu, G.; Eisenberg, A. *J. Membr. Sci.* **1993**, *82*, 83.
(37) Jiang, M.; Gronowski, A. A.; Yeager, H. L.; Wu, G.; Kim, J.-S.; Eisenberg, A. *Macromolecules* to be submitted.
(38) Eisenberg, A.; Navratil, M. *Macromolecules* **1973**, *6*, 604.
(39) Eisenberg, A.; Navratil, M. *Macromolecules* **1974**, *7*, 90.
(40) Hird, B.; Eisenberg, A. *J. Polym. Sci., Part B: Polym. Phys.* **1990**, *28*, 1665.
(41) Williams, M. L.; Landel, R. F.; Ferry, J. D. *J. Am. Chem. Soc.* **1955**, *77*, 3701.
(42) Kim, J.-S.; Yoshikawa, K.; Eisenberg, A. *Macromolecules*, submitted.
(43) Hird, B.; Eisenberg, A. *Macromolecules* **1992**, *25*, 6466.
(44) Boyer, R. F. *Macromolecules* **1973**, *6*, 288.
(45) Maurer, J. J. In *Thermal Analysis*; Miller, B., Ed.; John Wiley & Sons: New York, 1982; Vol. 2.
(46) Tong, X.; Bazuin, C. G. *Chem. Mater.* **1992**, *4*, 370.
(47) Kim, J.-S.; Wu, G.; Eisenberg, A. *Macromolecules* **1994**, *27*, 814.
(48) Kim, J.-S.; Roberts, S. B.; Eisenberg, A.; Moore, R. B. *Macromolecules* **1993**, *26*, 5256.
(49) Tong, X.; Bazuin, C. G. *J. Polym. Sci., Polym. Phys. Ed.* **1992**, *30*, 389.
(50) Takamatsu, T.; Eisenberg, A. *J. Appl. Polym. Sci.* **1979**, *24*, 2221.
(51) Weast, R. C.; Lide, D. R.; Astle, M. J.; Beyer, W. H., Eds. *CRC Handbook of Chemistry and Physics*, 70th ed.; CRC Press: Boca Raton, FL, 1989.
(52) Brandrup, J.; Immergut, E. H., Eds. *Polymer Handbook*; John Wiley & Sons: New York, 1988.
(53) Arai, K.; Eisenberg, A. *J. Macromol. Sci., Phys.* **1980**, *B17*, 803.
(54) Nielsen, L. E. *Rheol. Acta* **1974**, *13*, 86.
(55) Lewis, T. B.; Nielsen, L. E. *Trans. Soc. Rheol.* **1968**, *12*, 421.
(56) Feng, S.; Sen, P. N. *Phys. Rev. Lett.* **1984**, *52*, 216.
(57) Kantor, Y.; Webman, I. *Phys. Rev. Lett.* **1984**, *52*, 1891.
(58) Benguigui, L. *Phys. Rev. Lett.* **1984**, *53*, 2028.
(59) Sahimi, M. *J. Phys. C: Solid State Phys.* **1986**, *19*, L79.
(60) Forsman, J.; Harrison, J. P.; Rutenberg, A. *Can. J. Phys.* **1987**, *67*, 767.
(61) Gauthier-Manuel, B.; Guyon, E. *J. Phys. (Paris), Lett.* **1980**, *41*, L503.
(62) Adam, M.; Delsanti, M.; Durand, D.; Hild, G.; Munch, J. P. *Pure Appl. Chem.* **1981**, *53*, 1489.
(63) Tokita, M.; Niki, R.; Hikichi, K. *J. Phys. Soc. Jpn.* **1984**, *53*, 480.
(64) Phani, M. K.; Dhar, D. *J. Phys. A* **1984**, *17*, L645.